



Phosphorothioated DNA Is Shielded from Oxidative Damage

Tianning Pu,^a Jingdan Liang,^a Zhiling Mei,^b Yan Yang,^a Jialiang Wang,^a Wei Zhang,^a Wei-Jun Liang,^c Xiufen Zhou,^a Zixin Deng,^a Zhijun Wang^a

^aState Key Laboratory of Microbial Metabolism, School of Life Science and Biotechnology, Shanghai Jiao Tong University, Shanghai, People's Republic of China

^bInstitute of Plant Physiology and Ecology, Shanghai Institutes for Biological Sciences, Chinese Academy of Sciences, Shanghai, People's Republic of China

^cDepartment of Life and Environmental Sciences, Faculty of Science and Technology, Bournemouth University, Poole, United Kingdom

ABSTRACT

Phosphorothioated DNA (PT-DNA) is a synthetic DNA analog in which one of the non-bridging phosphate groups in the DNA backbone is replaced by a sulfur atom. PT-DNA is known to be resistant to degradation by nucleases and to be more stable than natural DNA. In this study, we investigated the oxidative stability of PT-DNA. We found that PT-DNA is highly resistant to oxidative damage by hydrogen peroxide (H₂O₂) and hydroxyl radicals (•OH). The half-life of PT-DNA in the presence of H₂O₂ was 10.58 ± 0.90 min, while that of natural DNA was 2.419 ± 0.59 min. The half-life of PT-DNA in the presence of •OH was 31.03 min, while that of natural DNA was 0.1 min. The resistance of PT-DNA to oxidative damage was observed in both *Escherichia coli* and *Salmonella enterica*. The results suggest that PT-DNA is a promising candidate for applications in biotechnology and medicine.

IMPORTANCE

Phosphorothioated DNA (PT-DNA) is a synthetic DNA analog in which one of the non-bridging phosphate groups in the DNA backbone is replaced by a sulfur atom. PT-DNA is known to be resistant to degradation by nucleases and to be more stable than natural DNA. In this study, we investigated the oxidative stability of PT-DNA. We found that PT-DNA is highly resistant to oxidative damage by hydrogen peroxide (H₂O₂) and hydroxyl radicals (•OH). The half-life of PT-DNA in the presence of H₂O₂ was 10.58 ± 0.90 min, while that of natural DNA was 2.419 ± 0.59 min. The half-life of PT-DNA in the presence of •OH was 31.03 min, while that of natural DNA was 0.1 min. The resistance of PT-DNA to oxidative damage was observed in both *Escherichia coli* and *Salmonella enterica*. The results suggest that PT-DNA is a promising candidate for applications in biotechnology and medicine.

KEYWORDS

phosphorothioated DNA, oxidative damage, hydrogen peroxide, hydroxyl radicals, *Escherichia coli*, *Salmonella enterica*

Citation Pu T, Liang J, Mei Z, Yang Y, Wang J, Zhang W, Liang W-J, Zhou X, Deng Z, Wang Z. 2019. Phosphorothioated DNA is shielded from oxidative damage. *Appl Environ Microbiol* 85:e00104-19. <https://doi.org/10.1128/AEM.00104-19>.

Editor M. Julia Pettinari, University of Buenos Aires

Copyright © 2019 American Society for Microbiology. All Rights Reserved.

Address correspondence to Zixin Deng, zxdeng@sjtu.edu.cn, or Zhijun Wang, wangzhijun@sjtu.edu.cn.

T.P. and J.L. contributed equally to this work.

Received 13 January 2019

Accepted 5 February 2019

Accepted manuscript posted online 8 February 2019

Published 4 February 2019

A (1). A
 A (2 4).
 A (5, 6). *Clostridium*
difficile, 60% (7).
Leptospira A (8), A 50%
Mycobacterium abscessus (9, 10).
 - (5, 6), -
Escherichia coli 7A *Salmonella enterica*
 87, 10⁴ ()
 (5). 10³
Vibrio (5). A
 A (11).
 5' 3') *E. coli* *Streptomyces lividans* AA /
 (12).
 A *in vitro* (13, 14).
 (14 16),
E. coli *S. enterica*
 (16). A
 (16).
E. coli (2 2⁻)
 (17 19).
 A () A.
 ()
 A 2 2

RESULTS

Fenton reaction of PT DNA.

2 2
 2 2 (1. . .) 2+ (100 μ.)
 (. . .)
 .1
 A ()
 A (m/z 581) - A (m/z 565) (15).
 A (13),
 A

Preferential complexation of DndCDE to PT DNA.

A
E. coli -
 (2 2⁻) (17)
 1655 (17). A
in vivo 2 2⁻
S. enterica 87 *E. coli*.
 dndCDE

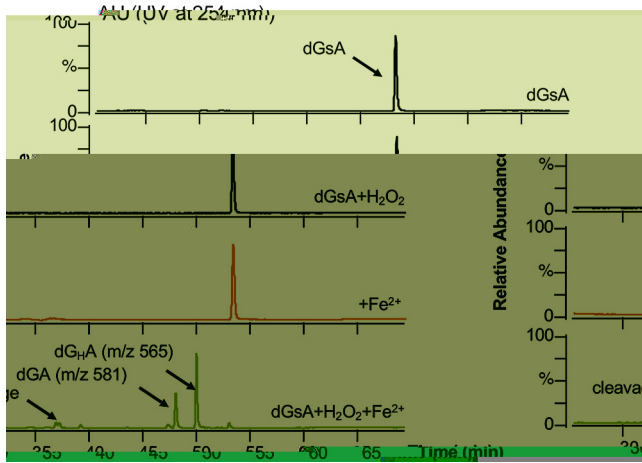


FIG 1

()₂ ()₂ A

1. 2 2 100 μ

() () 2A, ()

440 880 () 2A, ()

440 880 () 2A, () 2.

() A).

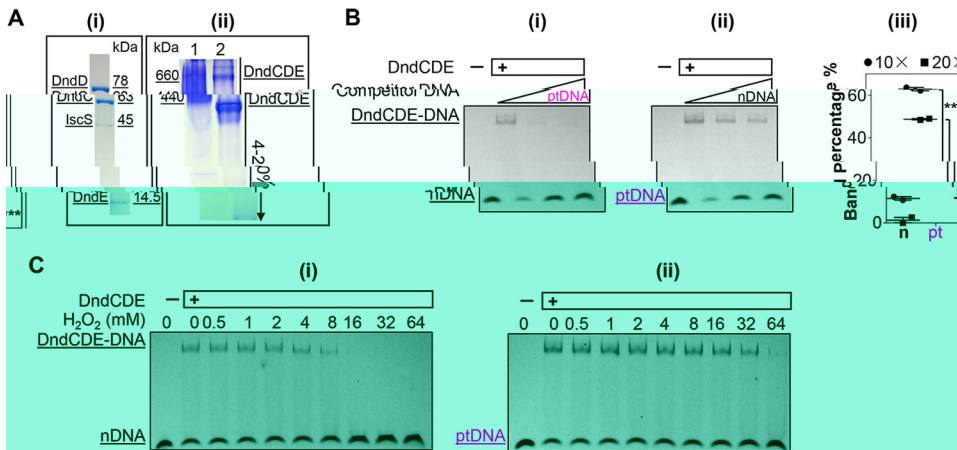


FIG 2

() / ()

1, 2 μ

() A

() A

() A

() A

() A

() A

() A

A

A

A

A

A

A

A

A

A

A

A

A

A

A

A

A

A

A

A

A

A

A

A

A

A

A

A

A

A

A

A

A

A

A

A

A

A

A

A

A

A

A

A

A

A

A

A

A

A

A

A

A

A

A

A

A

A

A

A

A

A

A

A

A

A

A

A

A

A

A

A

A

A

A

A

A

A

A

A

A

A

A

A

A

A

A

A

A

A

A

A

A

A

A

A

A

A

A

A

A

A

A

A

A

A

A

A

A

A

A

A

A

A

A

A

A

A

A

A

A

A

A

A

A

A

A

A

A

A

A

A

A

A

A

A

A

A

A

A

A

A

A

A

A

A

A

A

A

A

A

A

A

A

A

A

A

A

A

A

A

A

A

A

A

A

A

A

A

A

A

A

A

A

A

A

A

A

A

A

A

A

A

A

A

A

A

A

A

A

A

A

A

A

A

A

A

A

A

A

A

A

A

A

A

A

A

A

A

A

A

A

A

A

A

A

A

A

A

A

A

A

A

A

A

A

A

A

A

A

A

A

A

A

A

A

A

A

A

A

A

A

A

A

A

A

A

A

A

A

A

A

A

A

A

A

A

A

A

A

A

A

A

A

A

A

A

A

A

A

A

A

A

A

A

A

A

A

A

A

A

A

A

A

A

A

A

A

A

A

A

A

A

A

A

A

A

A

A

A

A

A

A

A

A

A

A

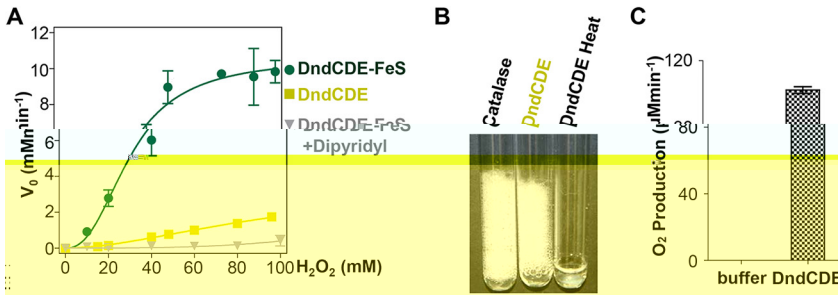


FIG 3 (A) Initial velocity (V_0) of H_2O_2 decomposition by DndCDE-FeS (green circles), DndCDE (yellow squares), and DndCDE-FeS + Dipyridyl (grey triangles) at various concentrations of H_2O_2 (0 to 100 mM). (B) Visual representation of H_2O_2 decomposition by Catalase, DndCDE, and DndCDE Heat. (C) O_2 production by DndCDE compared to buffer. Error bars represent standard deviation ($n = 3$).

DndCDE-FeS actively decomposes H_2O_2 .

(20, 21).
 (22).
 (23),
 (24, 25),
 (26).
 (27).
 (28).
 (29).
 (30).
 (31).
 (32).
 (33).
 (34).
 (35).
 (36).
 (37).
 (38).
 (39).
 (40).
 (41).
 (42).
 (43).
 (44).
 (45).
 (46).
 (47).
 (48).
 (49).
 (50).
 (51).
 (52).
 (53).
 (54).
 (55).
 (56).
 (57).
 (58).
 (59).
 (60).
 (61).
 (62).
 (63).
 (64).
 (65).
 (66).
 (67).
 (68).
 (69).
 (70).
 (71).
 (72).
 (73).
 (74).
 (75).
 (76).
 (77).
 (78).
 (79).
 (80).
 (81).
 (82).
 (83).
 (84).
 (85).
 (86).
 (87).
 (88).
 (89).
 (90).
 (91).
 (92).
 (93).
 (94).
 (95).
 (96).
 (97).
 (98).
 (99).
 (100).

H_2O_2 decomposition requires an intact DndCDE.

(101).
 (102).
 (103).
 (104).
 (105).
 (106).
 (107).
 (108).
 (109).
 (110).

Downloaded from <http://aem.asm.org/> on September 1, 2020 at Shanghai Jiao Tong University

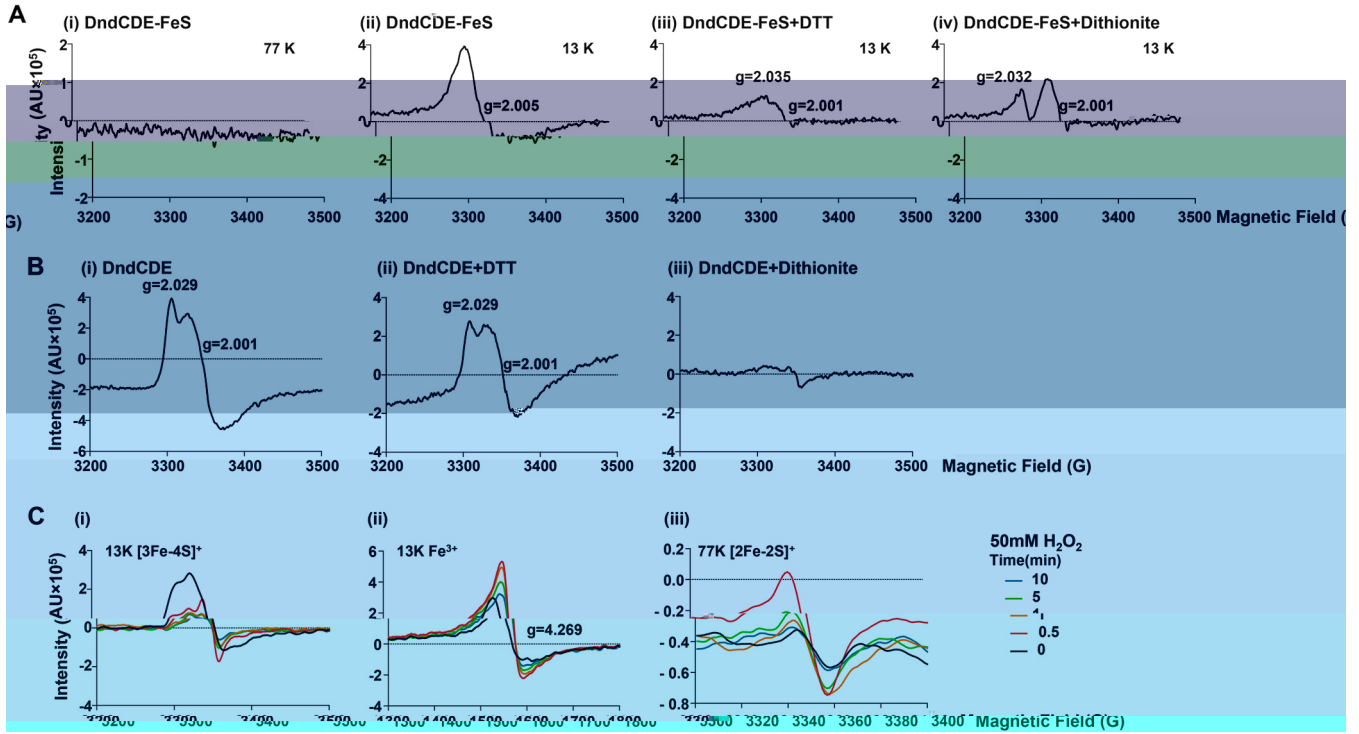


FIG 4

77, 13, 130 μ, 10/12, 2, -2, 3, -4, 4, -4, 2, 13, 0, 0.5, 1, 5, 10, (A), (B), (C), (D), (E), (F), (G), (H), (I), (J), (K), (L), (M), (N), (O), (P), (Q), (R), (S), (T), (U), (V), (W), (X), (Y), (Z), (AA), (AB), (AC), (AD), (AE), (AF), (AG), (AH), (AI), (AJ), (AK), (AL), (AM), (AN), (AO), (AP), (AQ), (AR), (AS), (AT), (AU), (AV), (AW), (AX), (AY), (AZ), (BA), (BB), (BC), (BD), (BE), (BF), (BG), (BH), (BI), (BJ), (BK), (BL), (BM), (BN), (BO), (BP), (BQ), (BR), (BS), (BT), (BU), (BV), (BW), (BX), (BY), (BZ), (CA), (CB), (CC), (CD), (CE), (CF), (CG), (CH), (CI), (CJ), (CK), (CL), (CM), (CN), (CO), (CP), (CQ), (CR), (CS), (CT), (CU), (CV), (CW), (CX), (CY), (CZ), (DA), (DB), (DC), (DD), (DE), (DF), (DG), (DH), (DI), (DJ), (DK), (DL), (DM), (DN), (DO), (DP), (DQ), (DR), (DS), (DT), (DU), (DV), (DW), (DX), (DY), (DZ), (EA), (EB), (EC), (ED), (EE), (EF), (EG), (EH), (EI), (EJ), (EK), (EL), (EM), (EN), (EO), (EP), (EQ), (ER), (ES), (ET), (EU), (EV), (EW), (EX), (EY), (EZ), (FA), (FB), (FC), (FD), (FE), (FF), (FG), (FH), (FI), (FJ), (FK), (FL), (FM), (FN), (FO), (FP), (FQ), (FR), (FS), (FT), (FU), (FV), (FW), (FX), (FY), (FZ), (GA), (GB), (GC), (GD), (GE), (GF), (GG), (GH), (GI), (GJ), (GK), (GL), (GM), (GN), (GO), (GP), (GQ), (GR), (GS), (GT), (GU), (GV), (GW), (GX), (GY), (GZ), (HA), (HB), (HC), (HD), (HE), (HF), (HG), (HH), (HI), (HJ), (HK), (HL), (HM), (HN), (HO), (HP), (HQ), (HR), (HS), (HT), (HU), (HV), (HW), (HX), (HY), (HZ), (IA), (IB), (IC), (ID), (IE), (IF), (IG), (IH), (II), (IJ), (IK), (IL), (IM), (IN), (IO), (IP), (IQ), (IR), (IS), (IT), (IU), (IV), (IW), (IX), (IY), (IZ), (JA), (JB), (JC), (JD), (JE), (JF), (JG), (JH), (JI), (JJ), (JK), (JL), (JM), (JN), (JO), (JP), (JQ), (JR), (JS), (JT), (JU), (JV), (JW), (JX), (JY), (JZ), (KA), (KB), (KC), (KD), (KE), (KF), (KG), (KH), (KI), (KJ), (KL), (KM), (KN), (KO), (KP), (KQ), (KR), (KS), (KT), (KU), (KV), (KW), (KX), (KY), (KZ), (LA), (LB), (LC), (LD), (LE), (LF), (LG), (LH), (LI), (LJ), (LK), (LL), (LM), (LN), (LO), (LP), (LQ), (LR), (LS), (LT), (LU), (LV), (LW), (LX), (LY), (LZ), (MA), (MB), (MC), (MD), (ME), (MF), (MG), (MH), (MI), (MJ), (MK), (ML), (MN), (MO), (MP), (MQ), (MR), (MS), (MT), (MU), (MV), (MW), (MX), (MY), (MZ), (NA), (NB), (NC), (ND), (NE), (NF), (NG), (NH), (NI), (NJ), (NK), (NL), (NM), (NO), (NP), (NQ), (NR), (NS), (NT), (NU), (NV), (NW), (NX), (NY), (NZ), (OA), (OB), (OC), (OD), (OE), (OF), (OG), (OH), (OI), (OJ), (OK), (OL), (OM), (ON), (OO), (OP), (OQ), (OR), (OS), (OT), (OU), (OV), (OW), (OX), (OY), (OZ), (PA), (PB), (PC), (PD), (PE), (PF), (PG), (PH), (PI), (PJ), (PK), (PL), (PM), (PN), (PO), (PP), (PQ), (PR), (PS), (PT), (PU), (PV), (PW), (PX), (PY), (PZ), (QA), (QB), (QC), (QD), (QE), (QF), (QG), (QH), (QI), (QJ), (QK), (QL), (QM), (QN), (QO), (QP), (QQ), (QR), (QS), (QT), (QU), (QV), (QW), (QX), (QY), (QZ), (RA), (RB), (RC), (RD), (RE), (RF), (RG), (RH), (RI), (RJ), (RK), (RL), (RM), (RN), (RO), (RP), (RQ), (RR), (RS), (RT), (RU), (RV), (RW), (RX), (RY), (RZ), (SA), (SB), (SC), (SD), (SE), (SF), (SG), (SH), (SI), (SJ), (SK), (SL), (SM), (SN), (SO), (SP), (SQ), (SR), (SS), (ST), (SU), (SV), (SW), (SX), (SY), (SZ), (TA), (TB), (TC), (TD), (TE), (TF), (TG), (TH), (TI), (TJ), (TK), (TL), (TM), (TN), (TO), (TP), (TQ), (TR), (TS), (TT), (TU), (TV), (TW), (TX), (TY), (TZ), (UA), (UB), (UC), (UD), (UE), (UF), (UG), (UH), (UI), (UJ), (UK), (UL), (UM), (UN), (UO), (UP), (UQ), (UR), (US), (UT), (UU), (UV), (UW), (UX), (UY), (UZ), (VA), (VB), (VC), (VD), (VE), (VF), (VG), (VH), (VI), (VJ), (VK), (VL), (VM), (VN), (VO), (VP), (VQ), (VR), (VS), (VT), (VU), (VV), (VW), (VX), (VY), (VZ), (WA), (WB), (WC), (WD), (WE), (WF), (WG), (WH), (WI), (WJ), (WK), (WL), (WM), (WN), (WO), (WP), (WQ), (WR), (WS), (WT), (WU), (WV), (WW), (WX), (WY), (WZ), (XA), (XB), (XC), (XD), (XE), (XF), (XG), (XH), (XI), (XJ), (XK), (XL), (XM), (XN), (XO), (XP), (XQ), (XR), (XS), (XT), (XU), (XV), (XW), (XX), (XY), (XZ), (YA), (YB), (YC), (YD), (YE), (YF), (YG), (YH), (YI), (YJ), (YK), (YL), (YM), (YN), (YO), (YP), (YQ), (YR), (YS), (YT), (YU), (YV), (YW), (YX), (YY), (YZ), (ZA), (ZB), (ZC), (ZD), (ZE), (ZF), (ZG), (ZH), (ZI), (ZJ), (ZK), (ZL), (ZM), (ZN), (ZO), (ZP), (ZQ), (ZR), (ZS), (ZT), (ZU), (ZV), (ZW), (ZX), (ZY), (ZZ), (AA), (AB), (AC), (AD), (AE), (AF), (AG), (AH), (AI), (AJ), (AK), (AL), (AM), (AN), (AO), (AP), (AQ), (AR), (AS), (AT), (AU), (AV), (AW), (AX), (AY), (AZ), (BA), (BB), (BC), (BD), (BE), (BF), (BG), (BH), (BI), (BJ), (BK), (BL), (BM), (BN), (BO), (BP), (BQ), (BR), (BS), (BT), (BU), (BV), (BW), (BX), (BY), (BZ), (CA), (CB), (CC), (CD), (CE), (CF), (CG), (CH), (CI), (CJ), (CK), (CL), (CM), (CN), (CO), (CP), (CQ), (CR), (CS), (CT), (CU), (CV), (CW), (CX), (CY), (CZ), (DA), (DB), (DC), (DD), (DE), (DF), (DG), (DH), (DI), (DJ), (DK), (DL), (DM), (DN), (DO), (DP), (DQ), (DR), (DS), (DT), (DU), (DV), (DW), (DX), (DY), (DZ), (EA), (EB), (EC), (ED), (EE), (EF), (EG), (EH), (EI), (EJ), (EK), (EL), (EM), (EN), (EO), (EP), (EQ), (ER), (ES), (ET), (EU), (EV), (EW), (EX), (EY), (EZ), (FA), (FB), (FC), (FD), (FE), (FF), (FG), (FH), (FI), (FJ), (FK), (FL), (FM), (FN), (FO), (FP), (FQ), (FR), (FS), (FT), (FU), (FV), (FW), (FX), (FY), (FZ), (GA), (GB), (GC), (GD), (GE), (GF), (GG), (GH), (GI), (GJ), (GK), (GL), (GM), (GN), (GO), (GP), (GQ), (GR), (GS), (GT), (GU), (GV), (GW), (GX), (GY), (GZ), (HA), (HB), (HC), (HD), (HE), (HF), (HG), (HH), (HI), (HJ), (HK), (HL), (HM), (HN), (HO), (HP), (HQ), (HR), (HS), (HT), (HU), (HV), (HW), (HX), (HY), (HZ), (IA), (IB), (IC), (ID), (IE), (IF), (IG), (IH), (II), (IJ), (IK), (IL), (IM), (IN), (IO), (IP), (IQ), (IR), (IS), (IT), (IU), (IV), (IW), (IX), (IY), (IZ), (JA), (JB), (JC), (JD), (JE), (JF), (JG), (JH), (JI), (JJ), (JK), (JL), (JM), (JN), (JO), (JP), (JQ), (JR), (JS), (JT), (JU), (JV), (JW), (JX), (JY), (JZ), (KA), (KB), (KC), (KD), (KE), (KF), (KG), (KH), (KI), (KJ), (KL), (KM), (KN), (KO), (KP), (KQ), (KR), (KS), (KT), (KU), (KV), (KW), (KX), (KY), (KZ), (LA), (LB), (LC), (LD), (LE), (LF), (LG), (LH), (LI), (LJ), (LK), (LM), (LN), (LO), (LP), (LQ), (LR), (LS), (LT), (LU), (LV), (LW), (LX), (LY), (LZ), (MA), (MB), (MC), (MD), (ME), (MF), (MG), (MH), (MI), (MJ), (MK), (ML), (MN), (MO), (MP), (MQ), (MR), (MS), (MT), (MU), (MV), (MW), (MX), (MY), (MZ), (NA), (NB), (NC), (ND), (NE), (NF), (NG), (NH), (NI), (NJ), (NK), (NL), (NM), (NO), (NP), (NQ), (NR), (NS), (NT), (NU), (NV), (NW), (NX), (NY), (NZ), (OA), (OB), (OC), (OD), (OE), (OF), (OG), (OH), (OI), (OJ), (OK), (OL), (OM), (ON), (OO), (OP), (OQ), (OR), (OS), (OT), (OU), (OV), (OW), (OX), (OY), (OZ), (PA), (PB), (PC), (PD), (PE), (PF), (PG), (PH), (PI), (PJ), (PK), (PL), (PM), (PN), (PO), (PP), (PQ), (PR), (PS), (PT), (PU), (PV), (PW), (PX), (PY), (PZ), (QA), (QB), (QC), (QD), (QE), (QF), (QG), (QH), (QI), (QJ), (QK), (QL), (QM), (QN), (QO), (QP), (QQ), (QR), (QS), (QT), (QU), (QV), (QW), (QX), (QY), (QZ), (RA), (RB), (RC), (RD), (RE), (RF), (RG), (RH), (RI), (RJ), (RK), (RL), (RM), (RN), (RO), (RP), (RQ), (RR), (RS), (RT), (RU), (RV), (RW), (RX), (RY), (RZ), (SA), (SB), (SC), (SD), (SE), (SF), (SG), (SH), (SI), (SJ), (SK), (SL), (SM), (SN), (SO), (SP), (SQ), (SR), (SS), (ST), (SU), (SV), (SW), (SX), (SY), (SZ), (TA), (TB), (TC), (TD), (TE), (TF), (TG), (TH), (TI), (TJ), (TK), (TL), (TM), (TN), (TO), (TP), (TQ), (TR), (TS), (TU), (TV), (TW), (TX), (TY), (TZ), (UA), (UB), (UC), (UD), (UE), (UF), (UG), (UH), (UI), (UJ), (UK), (UL), (UM), (UN), (UO), (UP), (UQ), (UR), (US), (UT), (UU), (UV), (UW), (UX), (UY), (UZ), (VA), (VB), (VC), (VD), (VE), (VF), (VG), (VH), (VI), (VJ), (VK), (VL), (VM), (VN), (VO), (VP), (VQ), (VR), (VS), (VT), (VU), (VV), (VW), (VX), (VY), (VZ), (WA), (WB), (WC), (WD), (WE), (WF), (WG), (WH), (WI), (WJ), (WK), (WL), (WM), (WN), (WO), (WP), (WQ), (WR), (WS), (WT), (WU), (WV), (WW), (WX), (WY), (WZ), (XA), (XB), (XC), (XD), (XE), (XF), (XG), (XH), (XI), (XJ), (XK), (XL), (XM), (XN), (XO), (XP), (XQ), (XR), (XS), (XT), (XU), (XV), (XW), (XX), (XY), (XZ), (YA), (YB), (YC), (YD), (YE), (YF), (YG), (YH), (YI), (YJ), (YK), (YL), (YM), (YN), (YO), (YP), (YQ), (YR), (YS), (YT), (YU), (YV), (YW), (YX), (YY), (YZ), (ZA), (ZB), (ZC), (ZD), (ZE), (ZF), (ZG), (ZH), (ZI), (ZJ), (ZK), (ZL), (ZM), (ZN), (ZO), (ZP), (ZQ), (ZR), (ZS), (ZT), (ZU), (ZV), (ZW), (ZX), (ZY), (ZZ)

Fe-S cluster and H₂O₂ decomposition. (22). 2, 3, 4, 2, -2, 3+, 4-, 2+, 3+. In vivo, 2, -2, 4, -4, 2, -2, 4, -4 (27). 77, 13, 2.005, g, 4A, 13, g, 4, -4, 4A, (27). 4, -4, (28, 29). 4, -4, 2+, 4, -4, + (29). 4, -4, 3+, 4, -4, 2+, 4, -4, 3+

Downloaded from <http://aem.asm.org/> on September 1, 2020 at Shanghai Jiao Tong University

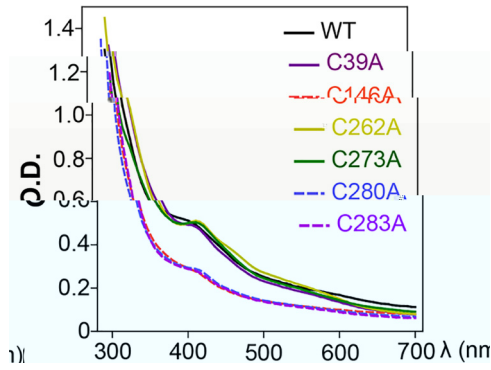


FIG 6

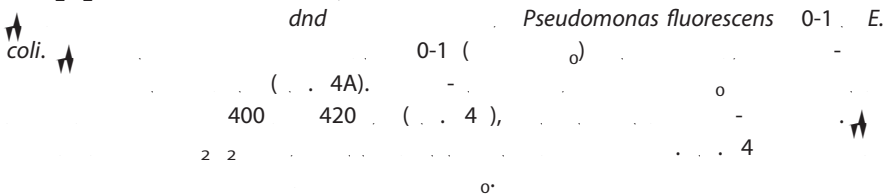
130 μ.

(λ₄₀₀).

Conserved cysteine residues in DndC participate in H₂O₂ decomposition.



H₂O₂ decomposition activity of DndCDE from *Pseudomonas fluorescens* Pf0-1.



DISCUSSION

E. coli *S. enterica*, 1,400
(5), 3.4
A
(16)
Salmonella enterica,
(37, 38)
() (39)
A
(...1).
(6, 40),
dndCDE
(17), A
A
Pseudomo-
nas fluorescens 0-1 (4A
) *S. enterica*, 2 2 ()
(41).
S. enterica

(A, A). (1, A);
 1% (A, A).
).
E. coli 10 (53).
dndC.
 (A) *E. coli* 21(3)/
 (A, A, A).
 (10 / , 5 /
 , 10 /)
 50 μ ⁻¹
 , *E. coli* 1
 50 μ ⁻¹ 37 250
 600 (600) 0.6. A
 ()
 0.1 ,
 24 16 . A 6,000 \times g
 20 -80

Protein expression and purification. (i) N-terminal His-tagged cysteine desulfurase, *IscS*.

(52). 1 50.
 (20. 8.0, 150. 5%) 50-
 (A) 100 μ 6.4-
 10. 2- 4- (500:
). 18,000 \times g 20 ,
 A), 10. (A) (A,
 5%). (20. 8.0, 150. , 40
 8.0, 150. , 500. , 5%), 2.5
 -10 (A, A) 3.5 (20. ,
 8.0, 150. , 5%)
 (54).

(ii) C-terminal His-tagged Dnd protein complex DndCDE or DndCDE_{PfO}.

() 5
) 50- ().
 - A 1- (;
), 8.0, 25. , 5%) 1 (20.
 , 8.0, 150. , 5%). 2 (20.
 (20. , 8.0, 500. , 5%), 5.
 A ()
 200 10/30 () 2.
 1- 280
 (λ_{280}). (3.)
 0.5 8,000 \times 4 2 (A ,
). 1 (20. ,
 8.0, 150. , 5%) 6 4 ,
 (54).

(iii) Gradient native gel electrophoresis detection of both native and cross-linked DndCDE.

(A, A) 20. () (55).
 (56). 4% 20%
 , 4% 20%
 1.2. ()
 , 49.5%;
 , 3% (/) , 5. 3 \times (75. 57.6.
), 100 μ 10% (/) (A), 10 μ
 (), 8.7. 6.
 (49.5% , 3% ; , 5. 3 \times (75.)
 57.6.), 3. , 75 μ 10% (/) A , 7.5 μ , 918 μ
 20% 4%
 (A600457-0500;
)

(iv) *In vitro* anaerobic enzymatic formation of active Fe-S cluster Dnd protein complex, DndCDE-FeS.
 () (23).
 20 μ . 30. 1.
 α, α' - 2. -10
 () 3.5.

4 2 (A 900 μ 0.5- 8,000 $\times g$ 20 μ .)
 (20 7.5 0.5 (λ)₂(λ)₂ 0.5 15,000 $\times g$
 8.0, 150 5%) 1 (-20 -10 ;
 4 10 () 0.5- ()
 A, A) 4

UV-Vis and EPR analysis of DndCDE and DndCDE-FeS.

(2; A) 5
 200- μ 130 μ 20 (20 8.0, 150 5%) 96- (3599; A)
 λ ₂₉₀ λ ₇₀₀
 ()
 130 μ (20 8.0, 150 5%)
 (2) (2)
 () 910
 () A ()
 ; 2 ; 9.387 ; 13 77 . 5
 (130 μ) 12 μ 5 2 2 1,200 μ 60 μ 2.5 8.0
 (200 μ)
 0.5 1 2 5 10

Fenton reaction and HPLC-MS detection of phosphorothioate DNA.

25 μ A (100- μ 100 μ 2 A (31).
 1 2 2 () 30 10 μ
) 18 A 1100 (250 4.6 ; 5- μ)
) 0.1% (A 0.1%
 30 0.1% 1% 13% 35.5 13% 30%
 20 1% 10 30 / λ _{254,4}
 325 3,100 m/z 597 (A), 565 (A),
 581 (A)
EMSAs. A (A) 2;
 (A) / (A) 5' 6-
 50 μ 400 μ A 500- μ
 (150 8.0, 50 240) 300 μ 100 μ 5 \times
 100 10 A
 20- μ A 2 μ 5' A (4 μ), 2 μ
 4 μ (4 μ) 2 μ (100)
 8.0, 1 1 0.1 -1 A, 50%)
 10 μ 6.67 μ
 40 10 μ A 3.96% (49.5%
 3% (44.5)
 44.5 1 A) 0.5 \times
 3000 ()

Measurement of DndCDE and DndCDE-FeS H₂O₂ decomposition activities. (i) Colorimetric assay.

2 2 100- μ 20
 8.0, 150 125 5% 40 2 2 ()
 1.67 μ (0.25 -⁻¹) 25
 20 5-
 1,000- (20 8.0, 150 5%)
 10 200 μ
 (A ;) (18, 57),
 30

λ_{595} 2^+ , 10 μ . 100 μ . 2 2 2

A (ii) Bubble test. (26)

-100 10 1. 10 μ . 3. 2 2

20. 8.0, 150, 125, 5% 1% -100. (26)

(iii) UV absorption. 96- () 2 ()

λ_{240} () λ_{240} (58). 0, 15, 20, 24, 30, 40, 48, 60, 80, 96, 120, 160, 200, 240. (100- μ) 20, 8.0, 150, 125, 5%, 1.67 μ . A 3- 2.

5 (, A, A). A, 1 μ , 2 μ , 4 μ , 8 μ , 16 μ , 32 μ , 64 μ , 128 μ . A

(iv) O₂ liberation rate measurement (pO₂ oxygen electrode). (59). (2-) 50 2 2

1.67 μ . 125 (8.0). 2

SUPPLEMENTAL MATERIAL

[:// . /10.1128/A .00104-19.](http://dx.doi.org/10.1128/A.00104-19)

SUPPLEMENTAL FILE 1, , 0.2 .

ACKNOWLEDGMENTS

2015 554203) (31470830, 21661140002, 91753123).

REFERENCES

1. 1982. A 257:6595 6599. 2000. ? A A 10:117 121. [:// . /10.1089/ .1200.10.117.](http://dx.doi.org/10.1089/1.2000.10.117)
3. A, 2014. () 9. 63:357 367. [:// . /10.1007/ 00262-014 -1518- .](http://dx.doi.org/10.1007/00262-014-1518-)
4. A 2015. (A) 2198. 1 (-1) 3 38:122 129. [:// . /10.14348/ .2015.2129.](http://dx.doi.org/10.14348/2015.2129)
5. 2011. A A A 108:2963 2968. [:// . /10.1073/ .1017261108.](http://dx.doi.org/10.1073/pnas.1017261108)
6. A, 2005. A 57:1428 1438. [:// . /10.1111/ .1365-2958.2005.04764. .](http://dx.doi.org/10.1111/1365-2958.2005.04764)
7. A A, 2005. A *Clostridium difficile*. 54:155 157. [:// . /10 .1099/ .0.45808-0.](http://dx.doi.org/10.1099/0.45808-0)
8. A A *Leptospira* 49:289 291. [:// . /10.1111/ .1472-765 .2009.02641. .](http://dx.doi.org/10.1111/1472-7652.2009.02641)

Downloaded from <http://aem.asm.org/> on September 1, 2020 at Shanghai Jiao Tong University

9. A, A, 2004. *Mycobacterium abscessus* A
42:5582 5587. // /10.1128/
42.12.5582-5587.2004.
10. 2013. A *Mycobacterium abscessus* A
159:2323 2332. //
/10.1099/ .0.070318-0.
11. A, 2014.
5:3951. // /
10.1038/ 4951.
12. 2007. A
A 35:2944 2954. // /10
.1093/ / 176.
13. A, 1988. *Streptomyces lividans* A
A 16:4341 4352.
// /10.1093/ /16.10.4341.
14. A, 1995. A
16:888 894. //
/10.1002/ .11501601149.
15. 2012. A
A 40:9115 9124. // /10.1093/ / 650.
16. 2017. A
13:888 894. // /10.1038/
.2407.
17. A

